



Sudan University of Sciences & Technology

College of Graduate Studies



Morphometric Assessment of Sella Trucica Among Sudanese Using Computed Tompography

تقييم شكل السرج التركي وقياسه لدي السودانيين باستخدام الاشعة المقطعية

A thesis Submitted for Partial Fulfillment for the Requirement of
M.Sc Degree in Diagnostic Radiology

Prepared by:

Nashwa Abdalmoaty Abdalrahman Basheer

Supervisor:

Dr. Hussein Ahmed Hassan

2017

الآية

بِسْمِ اللَّهِ الرَّحْمَنِ الرَّحِيمِ

أَقْرَأْ بِاسْمِ رَبِّكَ الَّذِي خَلَقَ (١) خَلَقَ الْإِنْسَانَ مِنْ عَلَقٍ (٢) أَقْرَأْ وَرَبُّكَ الْأَكْرَمُ (٣) الَّذِي عَلَّمَ بِالْقَلَمِ (٤)

عَلَّمَ الْإِنْسَانَ مَا لَمْ يَعْلَمْ (٥)

صدق الله العظيم

(سورة العلق: ١-٥)

Dedication

*Every work needs self effort as well as guidance and supporting of those who close
to you*

My humble effort I dedicate to my family and friends

Along with all hard working and respected teachers

Acknowledgement

I would like to express my sincere gratitude to my supervisor **Dr. Hussein Ahmed Hassan** for his guidance and valuable help during this study. My deepest gratitude extends to my colleague Mugtaba Alghazali Mohamed, for his ultimate help and contentions support.

Abstract

This is descriptive retrospective study aimed to assess sella truciica morphmerty among Sudanese using computed tomography.

The study was done in ALZAYTOUNA specialist hospital PACS, sixty healthy subjects selected randomly. 30 males and 30 females, their age was from 1 yrs to more than 60 yrs. The measurement of SL, SW, SHA, SHM, SHP, SD and AP were reported. SPSS used to calculate mean and STD deviation and find correlation.

The study found 39 subjects (64.7%) were deep sella morphology and 21 subjects (35.2%) were shallow. The mean and STD deviation of SL, SW, SHA, SHM, SHP, SD and AP was (9.2 ± 2.0 mm), (9.6 ± 2.0 mm), (7.8 ± 1.7 mm), (8.3 ± 1.5 mm) and (7.7 ± 1.7 mm) respectively. Also the study found significant correlation between age and sella truciica measurement parameters. The SL *R* value 0.451, SW *R* value 0.600, SD *R* value 0.566 and AP *R* value 0.580.

The study concluded that the mean and STD of male SL (9.6 ± 2.4 mm) and for female (8.8 ± 1.6 mm) and mean and STD for age group (1-10) SL (7.5 ± 1.1 mm), (10-20) (8.9 ± 1.7 mm), (20-30) (9.2 ± 1.5 mm), (30-40) (11.4 ± 3.5 mm), (40-50) (8.3 ± 1.8 mm), more than 60 (10.2 ± 1.2 mm). Also the study concluded that wide variation in sella truciica morphology.

The study recommended further studies for sella truciica measurement and morphology in a large sample of Sudanese.

المستخلص

هذه الدراسة وصفية باثر رجعي هدفت إلى تقييم السرج التركي وقياسه لدى السودانيين باستخدام الاشعة المقطعية. وقد أجريت الدراسة في ارشيف مستشفى الزيتونة التخصصي، علي ٦٠ مريض مختارة عشوائيا ٣٠ من الذكور و ٣٠ من الإناث، وكان عمرهم من سنة إلى أكثر من ٦٠ عاما. تم تدوين قياس طول السرج التركي، العرض، الارتفاع الامامي، الارتفاع الاوسط، الارتفاع الخلفي، العمق والطول الامامي الخلفي. تم استخدام الحزمة الاحصائية للعلوم الاجتماعية لحساب المتوسط والانحراف المتوسط لايجاد معامل الارتباط.

وجدت الدراسة أن ٣٩ شخصا (٦٤.٧٪) كان شكل السرج التركي لديهم عميق و ٢١ شخصا (٣٥.٢٪) كان غير عميق. وكان المتوسط والانحراف المتوسط من طول السرج التركي، العرض، الارتفاع الامامي، الارتفاع الاوسط، الارتفاع الخلفي، العمق وطول الامامي الخلفي (٩.٢ ± ٢ مم)، (٩.٦ ± ٢ مم)، (٧.٨ ± ١٠.٧ مم)، (٨.٣ ± ١.٥ مم) و (٧.٧ ± ١.٧ مم) على التوالي. كما اوجدت الدراسة علاقة ارتباط قوي بين R value العرض ٠.٦٠٠ حيث كان طول السرج التركي ٠.٤٥١ العمر وعوامل القياس للسرج R value العمق ٠.٥٦٦ ، R value والطول الامامي الخلفي ٠.٥٨٠.

خلصت الدراسة إلى أن المتوسط والانحراف المتوسط لطول السرج التركي في الذكور (٩.٦ ± ٢.٤ مم) والإناث (٨.٨ ± ١.٦ مم) والمتوسط والانحراف المتوسط للفئة العمرية (١٠-١) لطول السرج التركي (٢.٧ ± ١.١ مم)، (٢٠-١٠) (٨.٩ ± ١.٧ مم)، (٣٠-٢٠) (٩.٢ ± ١.٥ مم)، (٤٠-٣٠) (١١.٤ ± ٣.٥ مم)، (٥٠-٤٠) (٨.٣ ± ١.٨ مم)، أكثر من ٦٠ (١٠.٢ ± ١.٢ مم). كما خلصت الدراسة إلى أن الاختلاف الكبير في شكل السرج التركي.

. أوصت الدراسة بمزيد من الدراسات لقياس السرج التركي وشكله في عينة كبيرة من السودانيين

List of contents

Content	Page
الإية	I
Dedication	II
Acknowledgement	III
Abstract (English)	IV
Abstract (Arabic)	V
List of contents	VI
List of abbreviations	VIII
List of tables	IX
List of figures	X
Chapter one	
Introduction	1
Chapter two	
Theoretical background	3
Previous studies	16
Chapter three	
Material and method	19
Chapter four	
Study results	22
Chapter five	
Discussion	29
Conclusion	31
Recommendation	32
References	33
Appendix A	
Appendix B	

List of abbreviations

ACTH	Adernocorticotropic Hormone
ADH	Antidiuetic Hormone
ANOVA	Analysis of Variance test
AP	Anteroposterior
Cm	Centimeter
CSF	Cerebrospinal Fluid
CPR	Curved Planar Reformation
CT	Computed Tomography
CVA	Cerebrovascular accident
DS	Dorsum Sella
FH	Frankfort Horizontal
FOV	Field of View
FSH	Follicle-stimulating Hormone
GH	Growth Hormone
IOML	Infera-orbital meatl line
Kg	Kilogram
LH	Luteinizing Hormone
LSD	Low Contrast Detectability
Mm	Millimeter
MPR	Multiplaner Reconstruction
PACS	Picture archiving communicating system
PRL	Prolactin
P value	Person value

SD	Sella Depth
SHA	Sella Height Anterior
SHM	Sella Height Median
SHP	Sella Height Posterior
SL	Sella Length
SM	Sella Morphology
SPSS	Statistical Package for Social Sciences
SR	Surface Rendering
SSD	Shaded Surface Display
STD	Stander Deviation
SW	Sella Width
TS	Tuberculum Sella
TSH	Thyroid Stimulating Hormone
VR	Volume Rendering
WL	Window level
WW	Window width
Yrs	Years old
2D	2 Dimension
3D	3 Dimension

List of Tables

(4-1)	Represents frequency distribution of gender
(4-2)	Represents frequency distribution of age
(4-3)	Frequency distribution of sella truca morphology
(4-4)	Represents compared mean of sex and sella truca measurements
(4-5)	Represents compared mean of age groups and sella truca measurements
(4-6)	Represents crosstabulation of sex and sella truca morphology
(4-7)	Represents correlation of age and sella truca length
(4-8)	Represents correlation of age and sella truca width
(4-9)	Represents correlation of age and sella truca depth
(4-10)	Represents correlation of age and sella truca anteroposterior diameter

List of Figures

2.1	Shows anatomy of sella trucaica
2.2	shows pituitary gland
2.3	Shows posterior pituitary hormone
2.4	Shows anterior pituitary hormone
2.5	Shows microadenoma
2.6	Shows macroadenoma
2.7	Shows Rathke's cleft cyst
2.8	Shows empty sella
2.9	Shows Meningioma
4.1	shows bar chart distribution of gender
4.2	Shows bar chart distribution of age
4.3	Shows bar chart distribution of sella trucaica morphology
4.5	Shows bar chart of sex and sella trucaica morphology

Chapter one

Introduction

Chapter one

1. Introduction

Sella tronica is a saddle-shaped depression located in the middle cranial fossa on the upper surface of the sphenoid bone. It is enclosed by the pituitary fossa in which the pituitary gland is lodged, tuberculum sellae on the front and dorsum sellae in the rear. Two anterior and two posterior clinoid processes form a protrusion on the pituitary fossa, and these are the structures that protect the pituitary gland in the sella tronica.(Devi et al 2013)

Research on sella tronica focuses not only on its dimensions, but also on its morphology. Sella morphology is important in both evaluating treatment outcomes and late developmental changes, and in assessing the cranial morphology. The anatomy of the sella tronica and clinoid processes may vary widely among individuals. Variations in sella tronica size are commonly observed and associated with the pathologies involving this region. (Turamanlar 2017)

Knowledge on the anatomy of the sellar region is important for neurologists and neurosurgeons in their assessments of the pathologies in this region. Acknowledgement of sellar area variations is also important in preventing injuries of the structures that surround the sella tronica during surgery. When surgeons are familiar with the variations, they can notice them during pre-operative radiological analyses. In addition, knowledge on potential variations may alter the choice of surgical technique, operative approach and surgical devices. (Devi et al 2013)

1-2Problem of study:

There are some controversies about a normal measurements and morphology of sella tronica.

1-3 Objective of study

1-3-1 General objective

To assess sella truca morphmerty using computed tomography for Sudanese.

1-3-2 Specific objective

To measure the normal sella truca in Sudan.

To describe sella truca shape.

To correlate the measurement with age.

To correlate the measurement with gender.

To compare it with pervious study.

1-4 Significant of study

The study attempt to create reference value of normal sella truca morphomerty.

1-5 Study overviews

Chapter one include introduction, study problem, objectives, significant of the study and overview. Chapter two includes theoretical background and previous studies. Chapter three includes materials and methods. Chapter four includes results. Chapter five includes discussions, conclusions, recommendations, references and appendix (A, B) showing the practical work.

Chapter two

Theoretical background and previous studies

Chapter two

Theoretical background and previous studies

2. Theoretical Background

2.1 Anatomy of sella truca

The sella truca, a saddle shaped depression in the upper surface of sphenoid bone is located between and bounded by the two anterior and two posterior clinoid processes. It is composed of three parts: the tuberculum sella, pituitary (or hypophysial) fossa which lodging the pituitary gland and the dorsum sella. (Snell 2008) (KS et al.2010)

The pituitary gland is covered on its superior surface by the diaphragma sella, which is a fold of dura matter attached to the anterior and posterior clinoid process. Central part of the diaphragma sella is pierced by an opening for pituitary stalk.(KS et al 2010)

The pituitary gland is covered on its superior surface by the diaphragma sella, which is a fold of dura matter attached to the anterior and posterior clinoid process. Central part of the diaphragma sella is pierced by an opening for pituitary stalk. (KS et al 2010).

The lesser wing of the sphenoid bone is prolonged posteromedially to form the anterior clinoid processes. The posterior clinoid processes are located at the superolateral angles of the dorsum sellae. Inconstant and variable the middle clinoid processes are located posterolateral to the tuberculum sella. Occasionally the anterior and posterior clinoid process may fuse to form what is termed as a sella truca bridge. Similarly, the middle clinoid process may at times be fused

with the anterior clinoid process by a thin and small bony spicule to form a caroticoclinoid foramen. (Snell 2008) (TS 1993) (CS 2004)

Three different positions of the pituitary stalk have been described: anterior when it is close to tuberculum sellae; middle when central to diaphragm sellae; posterior where it is close to dorsum sellae. Three different positions of the pituitary stalk have been described: anterior when it is close to tuberculum sellae; middle when central to diaphragm sellae; posterior where it is close to dorsum sellae. The diaphragma sellae, a small horizontal fold of dura that forms roof of pituitary when viewed from above has three different shapes: convex, concave, and flat diaphragma sellae has a central aperture of variable size, ranging from small foramen to a large hole which transmits the pituitary stalk and its blood vessels. (Dinc AH et al 2002) (HD et al 1972).

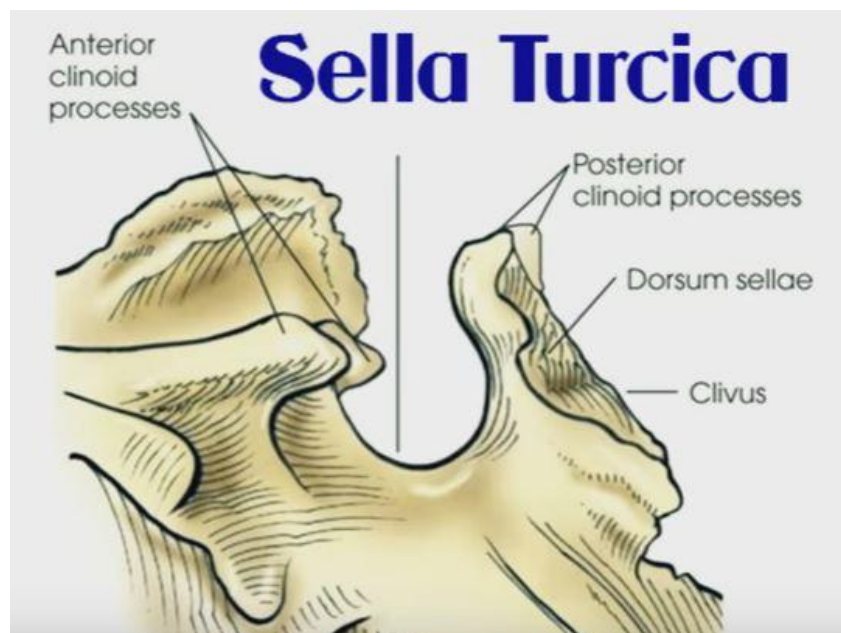


Fig (2.1) shows sella turcica anatomy. (HD et al 1972)

2-2 Physiology of sella region and pituitary gland

The hypothalamus–pituitary complex is located in the diencephalon of the brain. The hypothalamus and the pituitary gland are connected by a structure called the infundibulum, which contains vasculature and nerve axons.

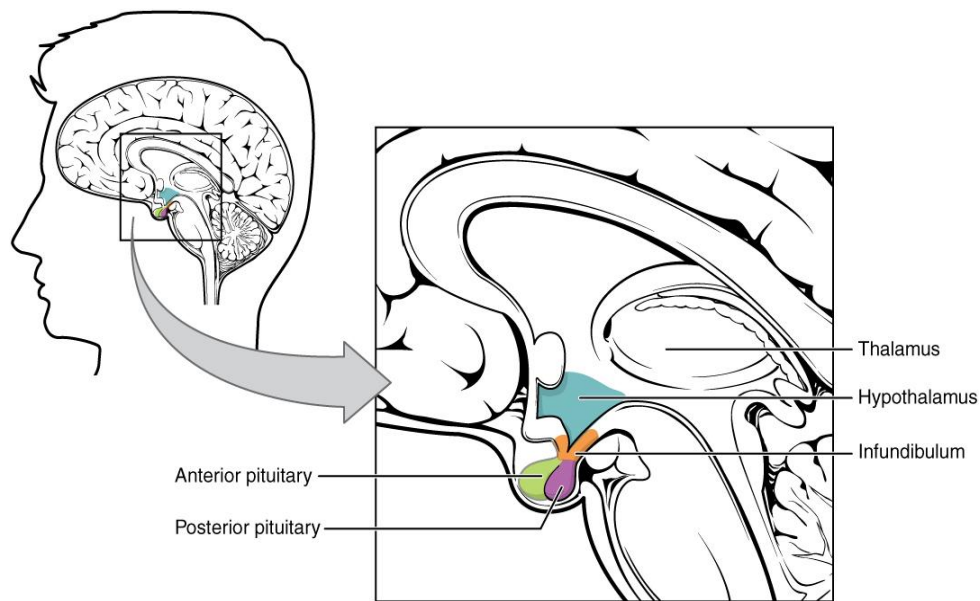


Fig (2.2) shows pituitary gland (wikibooks:image:human physiology)

The pituitary gland is divided into two distinct structures with different embryonic origins. The posterior lobe houses the axon terminals of hypothalamic neurons. It stores and releases into the blood stream two hypothalamic hormones: oxytocin and antidiuretic hormone (ADH). The anterior lobe is connected to the hypothalamus by vasculature in the infundibulum and produces and secretes six hormones. Their secretion is regulated, however, by releasing and inhibiting hormones from the hypothalamus. (David. 2007)

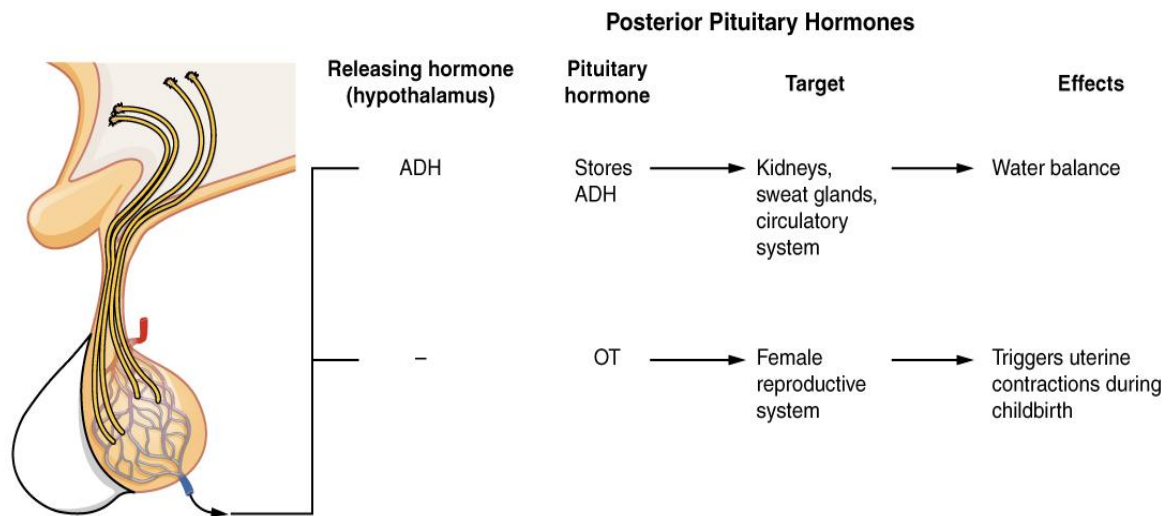


Fig (2.3) shows posterior pituitary hormones. (wikibooks:image:human physiology)

The six anterior pituitary hormones are: growth hormone (GH), thyroid-stimulating hormone (TSH), adrenocorticotrophic hormone (ACTH), follicle-stimulating hormone (FSH), luteinizing hormone (LH), and prolactin (PRL). (David 2007)

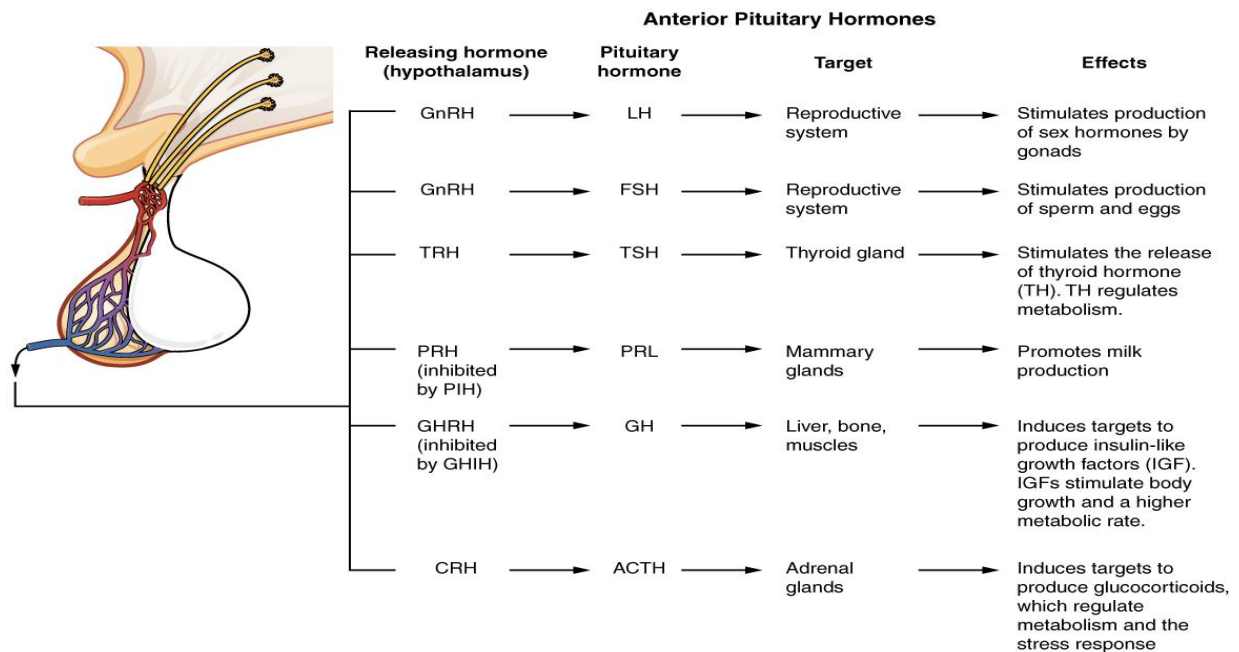


Fig (2.4) shows anterior pituitary hormones. (wikibooks:image:human physiology)

2-3 Pathology of sellar region and pituitary fossa

2-3-1 Congenital or developmental anomalies like pituitary hyoplasia

Are rare congenital anomalies and can be associated with septo-optic dysplasia, kallman syndrome, corpus callosum dysgenesis arnold chiari -I syndrome and commonly found in cases of pituitary dwarfism. Pituitary duplication is another rare congenital anomaly found in median cleft lip syndrome or frontonasal dysplasia. (Pathak 2015)

2-3-2 Microadenoma

Most common neoplasm of sella turcica, slow growing benign and essentially found in adults. As the name suggest these are small (less than 10 mm) in size. Clinical presentation depends upon whether it is hormonally active or nonfunctional adenoma. About 25% of microadenomas are hormonally inactive- hence called null cell adenomas; remaining 75% are hormonally active and produce excess hormone as per their cell of origin. The most common among them is prolactinoma- arising from the lactotrophs(50%). Other are ACTH secreting, TSH, LH& FSH secreting adenomas and pleurihormonal adenomas. The non-functioning adenomas generally present due to compression or invasion of adjacent structures. (Pathak 2015)

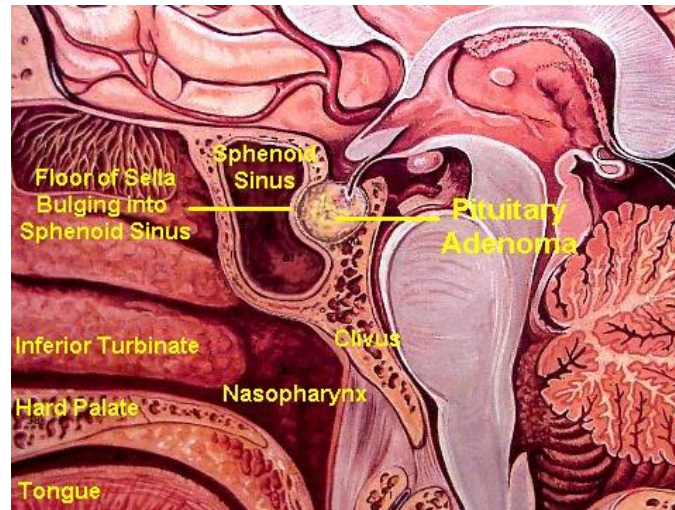


Fig 2-5 shows microadenoma. (Pathak 2015)

2-3-3Macroadenoas

Pituitary adenomas more than 10 mm in size are called macroadenomas. They generally present due to compressive symptoms on adjacent structures and usually nonfunctioning tumors. (Pathak 2015)

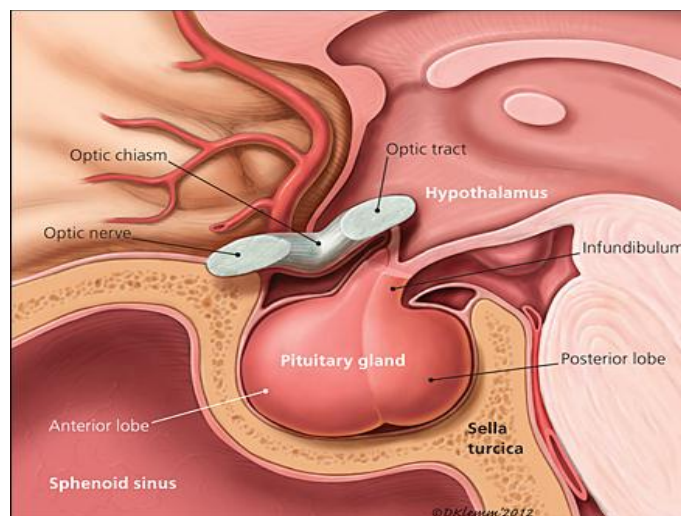


Fig 2-6 shows Macroadenoma. (Pathak 2015)

2-3-4 Rathke's cleft cyst

Is a developmental benign cystic lesion derived from squamous epithelium of Rathke's cleft. Has got no age predilection. It is predominantly intrasellar in location, occupies central part of the gland. May be found in suprasellar cistern in midline anterior to the pituitary stalk. Most are small and asymptomatic and discovered incidentally. It can become symptomatic if it enlarges sufficiently to cause pressure symptoms on pituitary gland or optic chiasm, rarely internal hemorrhage can occur when patients presents with headache. (Pathak 2015)

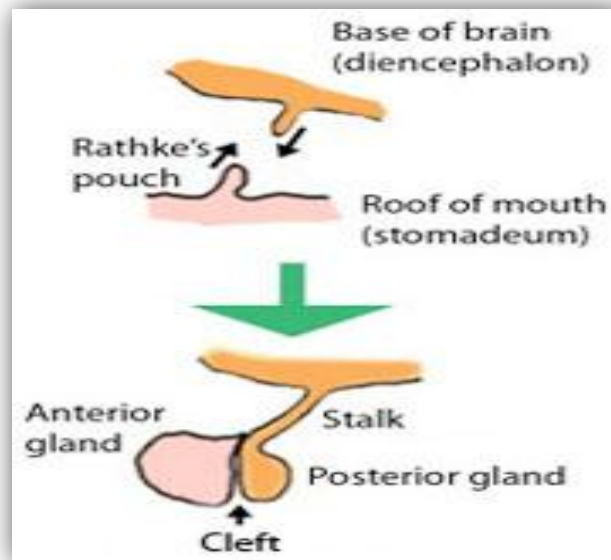


Fig 2-7 shows Rathke's cleft cyst. (Pathak 2015)

2-3-5 Empty sella

When the pituitary gland appears severely flattened against the sellar floor and most of the sella appears empty and occupied by CSF, it is called as empty sella. It may be an incidental finding or may present with nonspecific complaints like headache & dizziness. Only differential of empty sella is intrasellar arachnoid cyst. These two entities can be differentiated by looking at the pituitary stalk, which is in

midline in empty sella and displaced off midline in arachnoid cyst. (Pathak 2015)
(Pathak 2015)

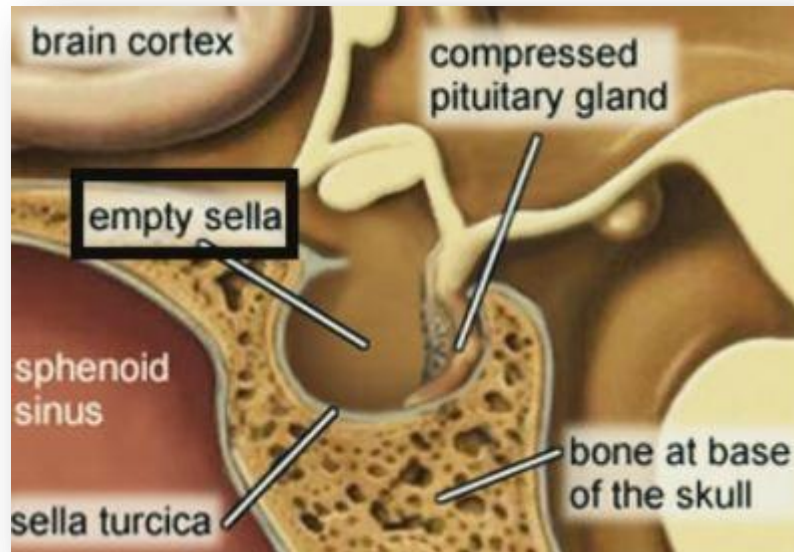


Fig 2-8 shows empty sella (Pathak 2015)

2-3-6 Meningioma

Common parasellar & suprasellar benign neoplasm which may extend inside the sella. It may arise from the tuberculum sellae, anterior clinoid process, planum sphenoidal and cavernous sinus. Slow growing neoplasms that present due to compression of adjacent structures. (JW et al 1988)

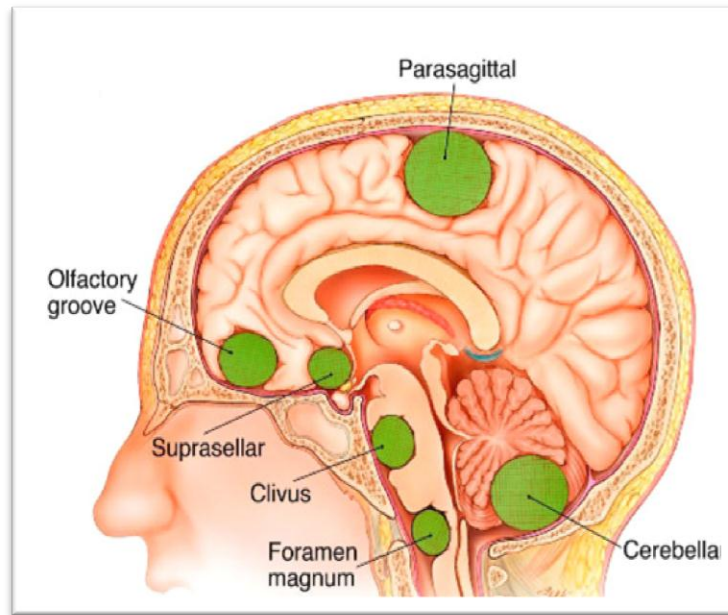


Fig 2-9 shows Meningioma. (Pathak 2015)

2-4 A 64 slice CT scanner background

The sole purpose of a CT scanner system is to produce diagnostic images and thereby aid a physician in the care and management of the patient. To accomplish this, the CT system must have, above all, superior image quality. There are many parameters that describe the quality of a CT image. These include low contrast detectability (LCD), spatial resolution, temporal resolution, noise, and various artifacts. In the end, it is the CT system's ability to faithfully represent the anatomy that defines its image quality. (Mather 2005)

Spiral or helical CT. Up to that time, power supply to the rotating gantry and data transmission out of the gantry was performed via cables. Therefore, the direction of rotation had to be reversed after each scan, substantially slowing down the acquisition of a series of images and making the system rather vulnerable for mechanical cable damages. These drawbacks were overcome with the introduction of slip ring technology for the power supply and optical transfer for data

transmission. The patient is moving slowly (1-3 mm/s) and continuously while the scanner rotates constantly at about 1-3 rotations/s. Spiral CT has the important advantage to be fast: modern scanners can collect and reconstruct a high-resolution slice of 512×512 pixels within half a second. (Demaio 1996)

2-4-1 Slip ring technology

It made spiral CT possible with normal gantry rotation is 1 revolution per second, although 0.5 s revolution is possible. The engineering required by stress of centrifugal force is formidable. Interpolation is the computation of an unknown value using known values on either side. Z-axis resolution is improved with 180° interpolation compared 360° interpolation. (Bushong 1976)

Extrapolation is the computation of an unknown value using known values on one side. 180° interpolation result in a thinner slice than 360° interpolations, 180° interpolations also result in a noiser image than 360° interpolations. (Bushong 1976)

Spiral-helical CT is made possible through the use of slip ring technology, which allows for continuous gantry rotation and result will be fast data collection. This technique is mandatory for such procedures as dynamic CT scanning. (Demaio1996)

The majority of slip ring technology is that facilitate continuous rotation of the x-ray tube, so that volume data can be acquired from the quickly. As the tube rotates continuously, the patient is translated continuously through the gantry aperture. This is result in CT scanning in spiral geometry. (Demaio 1996)

2-4-2 Data acquisitions

Multi-detector CT scanners with 16 or more slices are capable of routine acquisition of volumetric data sets in almost all patients, for all exams. Volumetric data sets are defined as data sets that have been acquired over a large amount of anatomy in a short time with isotropic (or near isotropic) voxels. An isotropic voxel is a cube, measuring the same in the x, y and z planes. (Mather 2005)

A typical single slice voxel has a dimension much longer in the z-axis than the x or y axis. This leads to adequate resolution in the plane of acquisition (usually axial) but poor quality images for MPR and 3D reconstructions. Isotropic voxels allow for true 3D imaging. No matter how the data set is projected there is no significant loss in resolution. Isotropic voxels are the essential building blocks for all types of advanced 3D and multiplanar visualization. Voxel size in the x and y dimension is dependent on the image matrix size and the field of view (FOV). (Mather 2005)

All current scanners routinely use a standard 512 X 512 image matrix; therefore, the only independent variable for x-y voxel size is the FOV. With a small FOV such as 25cm, the voxel size is 0.5mm. With a large FOV such as 50cm the voxel size is 1.0mm. The z-axis voxel size is determined by the slice thickness of the scan. Whenever possible slice thickness should match the voxel size in the x-y dimension as determined by the FOV. (Mather 2005)

2-4-3 Post processing tools

On helical data, image incrementation can be changed. This is often done to produce overlapping images that are then used in multiplanar or 3D reformations. When the slice thickness is wider or the FOV is larger, it is common practice to reconstruct images with an overlap of approximately 50% whenever multiplanar or

3D post-processing is expected to occur. For example, a case scanned with a slice thickness of 3.0 mm would be reconstructed every 1.5 mm. The decision as to whether overlapping slices may be beneficial depends on the voxel size in the specific study. When scans are generated with isotropic (or near isotropic) voxels, not much is gained from overlapping reconstructions. (Roman 2010)

Reformation that is done to show anatomy in various planes is referred to as multiplanar reformation (MPR). MPRs are 2D in nature. Unlike 3D displays, 2D image displays always represent the original CT attenuation values. MPRs can typically be created either at the operator's console or at a separate workstation. They can be created in transverse, coronal, sagittal, or oblique planes. Curved planar reformation (CPR) allows images to be created along the centerline of tubular organs. (Roman 2010)

The addition of special software allows another class of reformat to be performed. 3D reformation seeks to represent the entire scan volume in only one image. Unlike 2D displays, 3D techniques manipulate or combine CT values to display an image; the original CT value information is not included. For example, the technique known as surface rendering (SR) includes only information from the surface of an object. Because the 3D rendering process can be time-consuming, 3D software is generally available only on independent workstations so as to not tie up the operator's console. (Roman 2010)

Surface rendering (SR), also known as shaded-surface display (SSD), is similar to taking a photograph of the surface of the structure in that the voxels located on the edge of a structure are used to show the outline or outside shell of the structure. In most forms of SR, the images are created by comparing the intensity of each voxel in the data set to some predetermined threshold CT value. The software will

include or exclude the voxel depending on whether its CT number is above or below the threshold and use this information to create a surface of an object. The remaining voxels in the image are usually invisible. SR is useful (Roman 2010)

Volume rendering (VR) displays are built by collecting and manipulating data along a line from the viewer's eye through the data set. However, VR techniques sum the contributions of each voxel along the line. Each voxel is assigned an opacity value based on its Hounsfield units. This opacity value determines the degree to which it will contribute, along with other voxels along the same line, to the final image. The process is repeated for the voxels along each line, with each line producing one voxel in the VR image. Unlike other 3D techniques, with VR no information is ignored or discarded; every voxel contributes to the final image.(Roman 2010)

2-4-4 Sella trunca technique

The CT scan of sella trunca procedure is done to evaluate sella trunca and parasellar region. In order to perform the procedure patient positioned supine in the examination table with head place in the head holder, then centering the longitudinal alignment in midsagittal plane and transverse alignment above the infra- orbitometal line (IOML). Scan starting to obtain lateral as the scout at the beginning from 0.5 cm below hypophyseal region to ending in 0.5 cm above hypophyseal region. (Roman 2010)

Axial sequential mode of data acquisition is used for improved z-axis resolution which is excellent for a thinner slice thickness 2-3 mm and allow high quality helical examination of sella region. And volumetric acquisition also preferred whenever multiplaner reformation (MPR) or 3D imaging anticipated or when exam speed is a critical used. Additional image reconstruction with high spatial

frequency bone algorithm may be used maximize bony detail for suspected any abnormality. Sample window level and window width setting for optimal image display with soft tissue (WW 40-300. WL 30-40) and bone (WW 2000-3000, WL 200-400). (N 1996)

2-5 Previous studies

Turamanlai et al. 2017 they found Sella length was measured as 9.18 ± 1.91 mm, sella width 10.41 ± 1.74 mm, sella height anterior 8.09 ± 1.65 mm, sella height median 7.71 ± 1.24 mm, sella height posterior 7.48 ± 1.34 mm, sella area 69.15 ± 17.45 mm², sella depth 7.87 ± 1.37 mm and antero-posterior sella diameter as 11.48 ± 1.82 mm. When these sizes were compared between males and females, only sella length and width differed significantly. When compared by decades, there was a statistically significant difference only in the sella area parameter.

Mohamed et al. 2015 they found the pituitary stalk positions were middle in majority of male cases (72.7%), the remaining 27.3% were posterior. Among female; 57.1% were middle and the remaining 42.9% were posterior, no anterior position was detected among both genders with no different between male and female ($p = 0.494$) Normal Optic chiasma position was detected in all female cases and in 63.6% of male cases with no significant differences regarding gender ($p = 0.070$). No significant different in diaphragma sella shape and opening regarding gender (p .value = 0.170 and 0.914 respectively) No significant difference between males and females concerning linear dimensions of sella turcica (length, depth and Anteroposterior diameters). Concerning diaphragma sella opening; no significant different regarding gender in transverse diameter (p .value= 0.316) while significant different was detected in anteroposterior diameter (p .value= 0.046) for interclinoid (anterior, posterior) diameters, which represented statistically significant different

regarding gender in both right and left sides (p value = 0.004 and 0.001 respectively).

Devi et al.2013 they found the Percentage incidence of mid position of pituitary stalk is higher followed by posterior and anterior positions in both pre and postnatal groups. Three different positions of pre-fixed, post-fixed and normal of optic chiasma were observed in the present study. The percentage incidence of normal position was highest in both pre and postnatal cadavers. The percentage incidence of post-fixed is the next highest followed by prefixed. Three different shapes of diaphragm sella were observed and analysed sex-wise in the pre and post-natal cadavers in the present study. The shape of sellar opening was either elliptical or round with a higher incidence of round shape when compared to elliptical. One way ANOVA test for sella turcica and diaphragma sella parameters of aborted foetuses in the sample studied in various gestational age groups reveals that all the parameters are highly statistically significant with gestational age.

One way ANOVA carried out for various sella turcica and diaphragma sella parameters in foetuses with reference to sex reveals that only sella turcica depth is significant in different age groups with reference to sex whereas the other parameters are not significant. One way ANOVA carried out for various sella turcica and diaphragma sella parameters in post-natal sample of various age groups reveals that only sellar opening transverse diameter is significant with age. The remaining parameters are not significant. One way ANOVA carried out for various sella turcica and diaphragma sella parameters in post-natal cadavers with reference to sex reveals that only sella turcica depth is significant in different age groups with reference to sex whereas the other parameters are not significant.

Ruiz et al 2008 they found the sella turcica height varied from 2.9 mm to 11.1 mm, with a mean of 6.33 mm. Its length varied from 6 mm to 15.1 mm, with a mean of 10.31 mm. In respect of its area, this varied from 8 mm² to 79 mm², with a mean of 41.21 mm². In respect of its shape, the sella turcica was seen radiologically shown as three different shapes: in a U shape (48%), when the dorsum and tubercle of the sella turcica are maintained at the same height; in a J shape (41%), when the sella turcica tubercle is in a lower position in relation to the dorsum; and shallow (11%), when the sella turcica depth is minimum.

Amir 2013 he found the mean of the linear dimensions of the sella turcica in Sudanese were; (10.1 ± 1.6 mm) for length, (7.7 ± 1.8 mm) depth, and (11.8 ± 1.9 mm) for diameter. The sella turcica presented with a normal morphology in the majority of subjects (56 percent). No significant differences in linear dimensions between genders could be found (T values > 0.05). When age was evaluated, significant differences were found between the older and the younger age subjects, the sella length increases by 0.03mm starting from 8.9mm, the depth decreases by 0.04mm starting from 7.9mm, and the diameter increases by 0.02mm starting from 11.08mm, as the age increase by one year. When subject's height compared with the linear dimensions of sella the study found that the length increases by 0.02mm starting from 7.24mm, the depth increases by 0.01mm starting from 6.42mm, and the diameter increases by 0.02mm starting from 9.05mm, as the height increases by 1 cm. The study also found that the length increases by 0.04mm starting from 7.88mm, the depth increases by 0.02mm starting from 6.65mm, the diameter increases by 0.03mm starting from 10.23mm, as subject weight increases by 1kg.

Chapter three

Materials and Method

Chapter three

Materials and Method

3. Materials and Method

3-1 Materials

3-1-1 Design of study:

The study was retrospective and descriptive.

3-1-2 Area and duration of study:

This study was done in ALZAYTOUNA specialist hospital PACS. It was taking four months from March to July 2017.

3-1-3 Sampling and sample size:

Sampling was taken from patients who had normal CT brain, and sample size was sixty patients both male and female their age between 3yrs to 85 yrs.

3-1-4 Data collection:

Data collected by master sheets included age, gender, sella length (SL), sella width (SW), sella height anterior (SHA), sella height median (SHM), sella height posterior (SHP), sella depth (SD), antero-posterior (AP), sella morphology (SM).

3-2 Methods

3-2-1 Techniques

All CT examinations were performed by a 64 slice CT scanner (Aquillon 64, Toshiba medical systems, Tochigi, Japan) the images were reconstructed at mid-planner with slice thickness 3mm, then the mid-sagittal was zoomed, the

morphometric measurements were performed using eight parameters. The parameters were Sella Length (SL) whereas the distance between Tuberculum Sella (TS) and Dorsum Sella (DS) points. Sella Width (SW) from the most anterior and posterior points of sella trunca parallel to the Frankfort Horizontal plane (FH), whereas the FH was horizontal line drawn as base line at the bottom of sella trunca. Sella Height Anterior (SHA) the vertical distance measured from TS through sella trunca base to the FH plane. Sella height median (SHM) the vertical distance measured from the midpoint between TS and DS to the FH plane. Sella Height Posterior (SHP) the vertical distance measured from DS through sella trunca base to the FH plane. Sella trunca Depth (SD) the length of the line drawn vertically from the deepest point of the sella trunca in the direction of the sella trunca length. Sella trunca Antero-Posterior diameter (AP) the distance measured from the tuberculum sella to the backmost point in the interior surface of the posterior wall of the pituitary fossa. And sella morphology were observed and reported.

3-2-2 Inclusion criteria

Patients were from 3yrs to 85 yrs who had normal CT brain.

3-2-3 Exclusion criteria

Any patient had pathology in brain and cranial deformities, trans-nasal sphenoidal surgery.

3-2-3 Data analysis

Data were analyzed using IBM SPSS (Statistical Package for the Social Sciences, version 22.0; IBM, Chicago, IL, USA) software. Descriptive data were presented as mean \pm standard deviation, and correlations.

3-2-4 Ethical consideration

Maintained the confidentiality of the information

Chapter four

Results

Chapter four

Results

Table (4-1) represents frequency distribution of gender

		Frequency	Percent	Valid Percent	Cumulative Percent
Valid	male	30	50.0	50.0	50.0
	female	30	50.0	50.0	100.0
	Total	60	100.0	100.0	

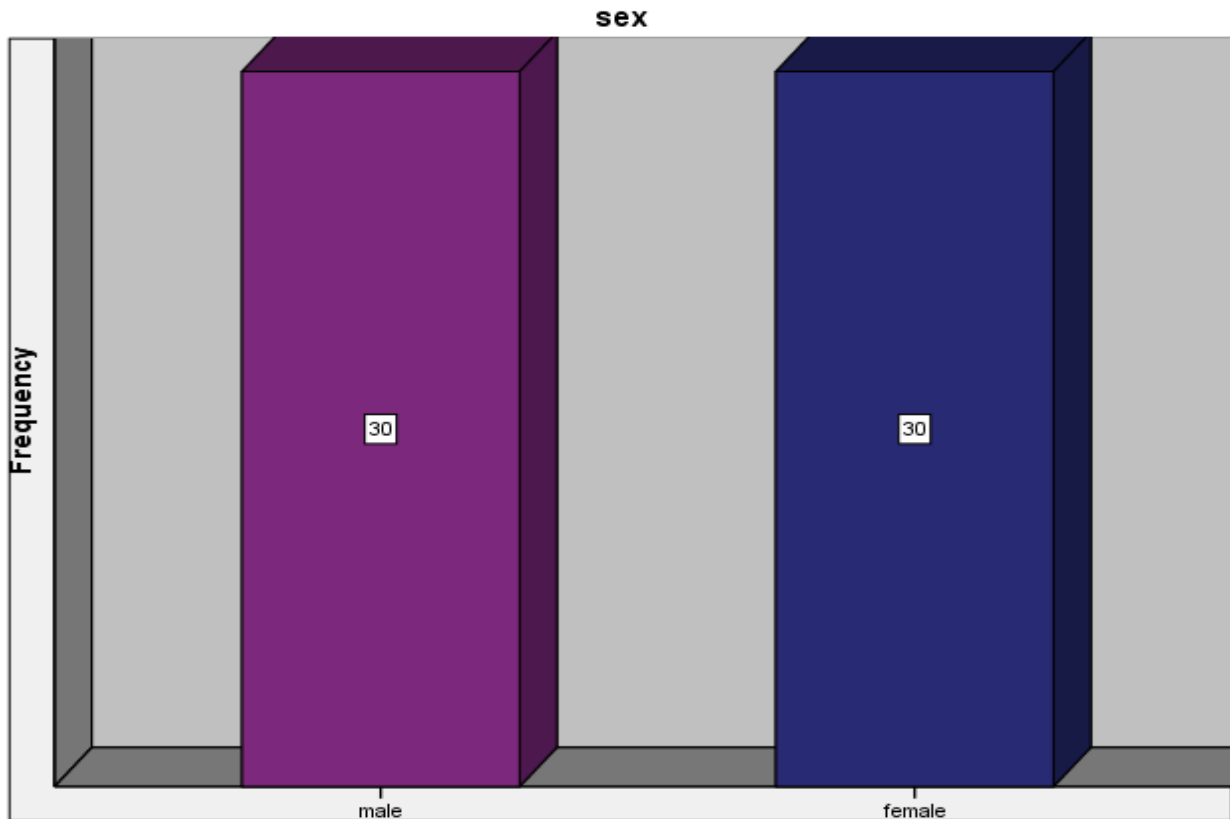


Fig (4.1) shows bar chart distribution of gender

Table (4-2) represents frequency distribution of age

		Frequency	Percent	Valid Percent	Cumulative Percent
Valid	1-10	15	24.9	25.0	25.0
	10-20	6	10.1	10.0	35.0
	20-30	8	13.4	13.3	48.3
	30-40	6	10.1	10.0	58.3
	40-50	6	10.1	10.0	68.3
	more than 60	19	31.4	31.7	100.0
	Total	60	100.0	100.0	

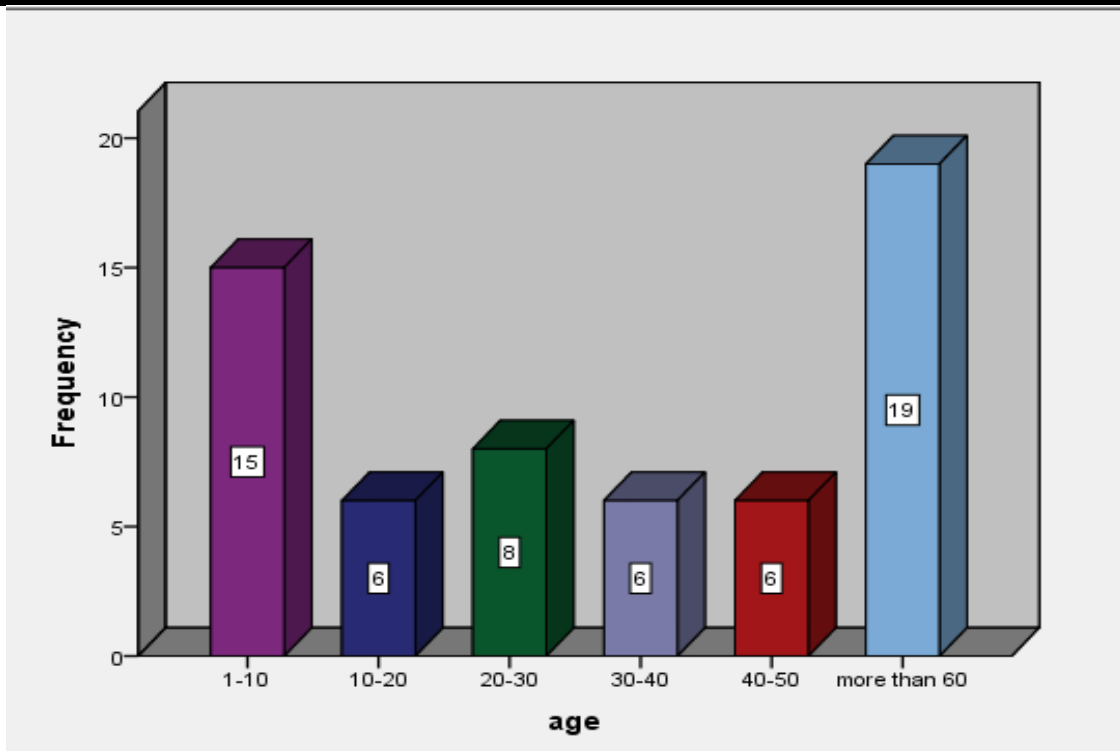


Fig (4.2) shows bar chart distribution of age

Table (4-3) represents frequency distribution of sella truca morphology

		Frequency	Percent	Valid Percent	Cumulative Percent
Valid	Deep	39	64.7	65.0	65.0
	Shallow	21	35.2	35.0	100.0
	Total	60	100.0	100.0	

SM

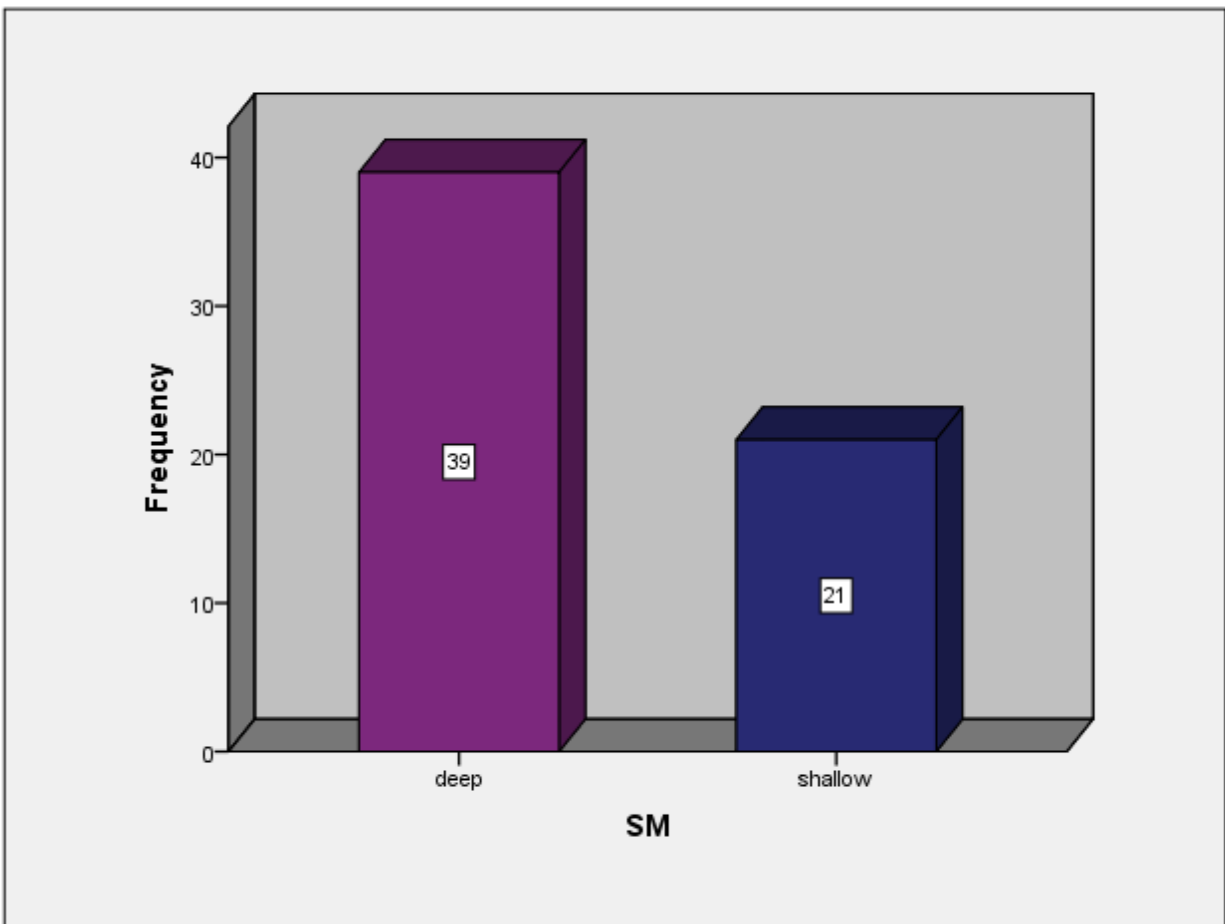


Fig (4.3) shows bar chart distribution of sella truca morphology

Table (4-4) represents compared mean of sex and sella truca measurements

Sex		SL	SW	SD
male	Mean	9.6000	9.3967	7.5833
	N	30	30	30
	Std. Deviation	2.43183	2.18876	1.96909
female	Mean	8.8700	10.0000	7.9000
	N	30	30	30
	Std. Deviation	1.60713	1.93409	1.40639
Total	Mean	9.2350	9.6983	7.7417
	N	60	60	60
	Std. Deviation	2.07649	2.07025	1.70396

Table (4-5) represents compared mean of age groups and sella truca measurements

Age		SL	SW	SD
1-10	Mean	7.5667	7.3133	5.8200
	N	15	15	15
	Std. Deviation	1.16353	1.70162	1.45022
10-20	Mean	8.9167	9.6500	8.1000
	N	6	6	6
	Std. Deviation	1.74059	1.18954	1.31605
20-30	Mean	9.2625	10.3000	8.0625
	N	8	8	8
	Std. Deviation	1.58559	1.06904	1.53431
30-40	Mean	11.4000	10.6333	8.1833
	N	6	6	6
	Std. Deviation	3.57043	2.03437	2.06244
40-50	Mean	8.3000	10.7167	8.9667
	N	6	6	6
	Std. Deviation	1.81769	1.64732	.78145
more than 60	Mean	10.2526	10.7263	8.4842
	N	19	19	19
	Std. Deviation	1.22537	1.54950	.90570
Total	Mean	9.2350	9.6983	7.7417
	N	60	60	60
	Std. Deviation	2.07649	2.07025	1.70396

Table (4-6) represents crosstabulation of sex and sella truca morphology

		SM		Total
		Deep	shallow	
Sex	male	21	9	30
	female	18	12	30
	Total	39	21	60

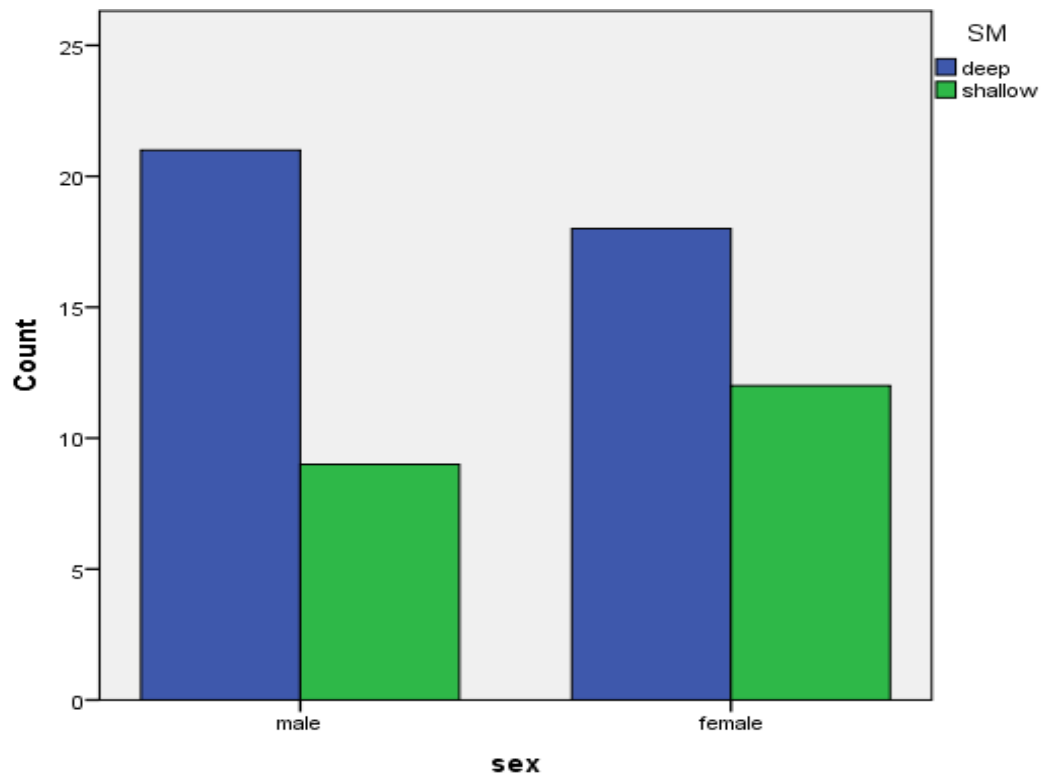


Fig (4-6) shows bar chart of sex and sella truca morphology

Table (4-7) represents correlation of age and sella truca length

		SL	Age
SL	Pearson Correlation	1	.451**
	Sig. (2-tailed)		.000
	N	60	60
Age	Pearson Correlation	.451**	1
	Sig. (2-tailed)	.000	
	N	60	60

**. Correlation is significant at the 0.01 level (2-tailed).

Table (4-8) represents correlation of age and sella truca width

		age	SW
Age	Pearson Correlation	1	.600**
	Sig. (2-tailed)		.000
	N	60	60
SW	Pearson Correlation	.600**	1
	Sig. (2-tailed)	.000	
	N	60	60

**. Correlation is significant at the 0.01 level (2-tailed).

Table (4-9) represents correlation of age and sella trucaica depth

		age	SD
Age	Pearson Correlation	1	.566**
	Sig. (2-tailed)		.000
	N	60	60
SD	Pearson Correlation	.566**	1
	Sig. (2-tailed)	.000	
	N	60	60

**. Correlation is significant at the 0.01 level (2-tailed).

Table (4-10) represents correlation of age and sella trucaica anteroposterior diameter

		age	AP
age	Pearson Correlation	1	.580**
	Sig. (2-tailed)		.000
	N	60	60
AP	Pearson Correlation	.580**	1
	Sig. (2-tailed)	.000	
	N	60	60

**. Correlation is significant at the 0.01 level (2-tailed).

Chapter five

Discussions and conclusion and recommendations

Chapter five

Discussions and conclusions and recommendations

5-1 Discussions

The study attempted to explain some controversies about normal measurement and morphology of sella truca. A 60 subjects 30 males and 30 females were selected randomly from PACS their age were grouped from 1 yrs to 85 yrs, the most age group were above 60 yrs due to more incident of cerebrovascular accident CVA and this results agree with Devi et al.2013. Table (4-2), fig (4.2).

Sella truca morphology was variety to as well as in both male and female. The study found the male had a deep sella truca shape was observed in deep represented 64.7% and male had the deepest shape than female. This result agrees with Devi et al .2013 and Ruiz et al.2008. Table (4-3),(4-6), fig 4.3, 4.6.

Sella truca measurement for age group was a variety in this study. The golden goal of this study is to create the reference measurement of sella truca for both male and female were (9.6 ± 2.0 mm), (8.9 ± 2.0 mm) respectively. This is result agree with Turamanlar O et al 2017 and disagree with scientific paper of Mohamed et al 2017. Due to a large sample of this study. Table (4-4).

The study found mean of measurements parameter of sella truca for different age group almost result of measurements parameter SL, SW, SD were agreed with all pervious study. Table (4-5)

Sella truca length (SL) was measured from TS to DS and profound mean was (9.3 ± 2.0 mm), SL correlated to age by person correlation coefficient, the study found significant correlation with value R 0.451 and this result agree with Turamanlar O et al 2017 and also agree with other scientific paper of Mohamed et al 2017 and Devi et al .2013. Table (4-7)

Sella truca width (SW) was measured from the most anterior and posterior point of ST parallel to FH and profound mean was (9.7 ± 2.0 mm), SW correlated to age by person correlation coefficient, the study found significant correlation with value p 0.600 and this result agree with Turamanlar O et al 2017 and also agree with other scientific paper of Mohamed et al 2017, and the SW mean disagree with Devi et al .2013. Table (4-8)

Table (4-9), (4-10) represents statistical descriptive and correlation of sella truca AP diameter and SD. The correlation with age were done by person correlation coefficient which had significant for both AP diameter and SD with value R 0.580 and 0.566 respectively and (mean and STD) (10.2 ± 2.2 mm) (7.8 ± 1.7 mm) respectively. This result agreed with Turamanlar O et al 2017 and also agree with other scientific paper of Mohamed et al 2017 and Devi et al .2013.

5-2 Conclusion

CT scan provides excellent spatial resolution to measure organ from acute edge to edge. The study concluded that the mean and STD of male SL (9.6 ± 2.4 mm) and for female (8.8 ± 1.6 mm) and mean and STD for age group (1-10) SL (7.5 ± 1.1 mm), (10-20) (8.9 ± 1.7 mm), (20-30) (9.2 ± 1.5 mm), (30-40) (11.4 ± 3.5 mm), (40-50) (8.3 ± 1.8 mm), more than 60 (10.2 ± 1.2 mm). Also the study concludes that wide variation in sella trunca morphology and there was significant correlation between SL and age groups with value R 0.451.

5-3 Recommendations

1. Further study recommended for sella tronica measurement and morphology in a large sample of Sudanese population.
2. Further study recommended for sella tronica measurement with more variables such as weight, height and head circumference.
3. Further study recommended for sella tronica measurement in specific ethnical group.

References

- Amir. 2013.Characterization and Measurement of Sella Turcica among Sudanese using CT. Sudan University of Science and Technology
- Aubrey David Nicholas. 2007. Human physiology European journal social sciences.
- Daniel N, Demaio. 1996 Mosby's exam review for computed tomography. New York.82-89.
- Devi et al.2013. Age and sex related morphology and morphometry of sellar region of sphenoid in prenatal and postnatal human cadavers. International Journal Research and Development of Health (. Int J Res Dev Health). VOL 1\ISSUE (3): 141 – 8.
- Gulsen S, Dinc AH, Unal M, Cantürk N, Altinors N. 2010. Characterization of the anatomic location of the Pituitary stalk and Its relationship to the Dorsum Sellae, Tuberculum Sellae and Chiasmatic Cistern, J Korean Neurosurg Soc. 47 :169-173.
- Ju KS, Bae HG, Park HK, Chang JC, Choi SK, Sim KM. 2010.Morphometric study of the Korean Adult Pituitary glands and the Diaphragma sellae Korean Neurosurg Soc. 2010.47.42-47).
- Kirgis HD, Locke W.1972 Anatomy and embryology. In: Locke W, Schally AV, editors. The hypothalamus and pituitary in health and disease. Springfield, IL. Charles C. Thomas. p. 3–65.
- Lois E. Romans. 2010. Computed tomography for technologists. Wolters kluwer health.
- Mohamed et al. 2015. A morphometric study of the sella turcica; gender effect. International Journal of Anatomy and Research (Int J Anat Res). VOL 3(1):927-34. ISSN 2321- 4287.
- Ranganathan TS,In 1993 . Text Book of Human Anatomy 5th Ed. S Chand and Company,New Delhi.528- 529.

Rhoton AL.2002. The sellar region. Neurosurgery. Journal of neurosurgery 51: S335- S374).

Richard Mather. 2005. Clinical Advancements in Volumetric CT. Springfield.63-69

Ruiz et al. 2008. Sella turcica morphometry using computed tomography. European Journal Anatomy (Eur J Anat). VOL12\ISSUE 1.47-50.

S. Pathak; Kalyan/IN. 2015 MRI imaging of sellar and suprasellar pathologies a pictorial assay. European society of radiology.p 3-6.

Sinnatamby CS.2004. Last's anatomy: Regional and Applied. Edinburgh. Churchill Livingstone.501-504.

Snell R S. 2008. The head and neck. In: Clinical Anatomy by Regions. 8 th ed.New York; Lippincott Williams and Wilkins.(667-850).

Stewart c. Bushong, sc.d, 1976 computed tomography essential of medical imaging. London

Turamanlai et al. 2017. morphometric assessment of sellaturcica using ct scan. Turkish society of clinical anatomy (TSACA). VOL. 11/ISSUE 1.

Yeakley JW, Kulkarni MV, McardleCB et al.1988. High resolution MR imaging of juxtaseilar meningiomas with CT & angiographic correlation AJNR Am J Neuroradiol. 9-279.

<http://wikibooks:image:human physiology>.

Appendix A

Table represents master data collection sheet

Age	sex	SL	SW	SHA	SHM	SHP	SD	SM	AP

Appendix B

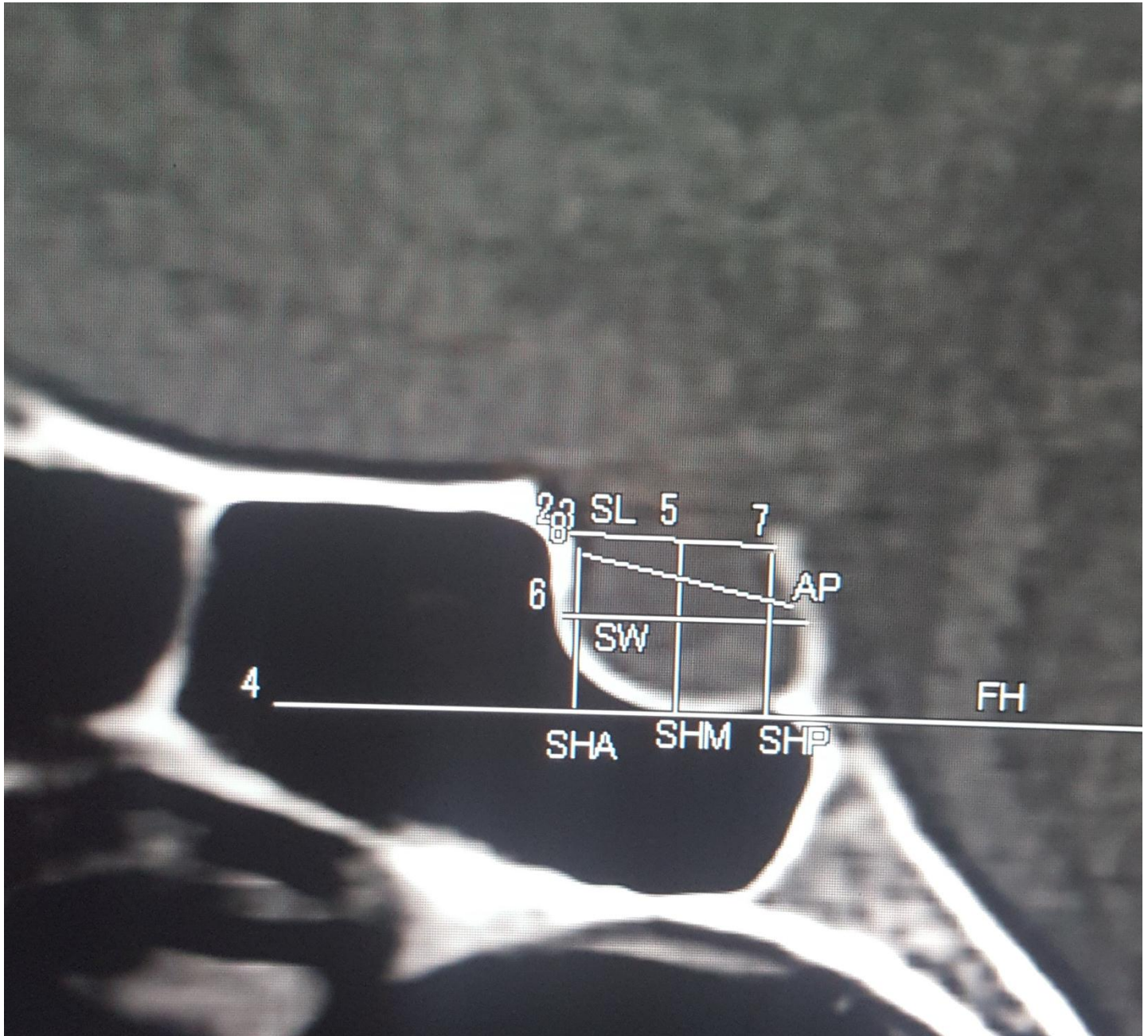


Fig mid sagittal CT scan of male 50 yrs. illustrate sella turcica measurements parameter and morphology